IEEE Access
Multidisciplinary | Rapid Review | Open Access Journal

Received 20 May 2024, accepted 3 June 2024, date of publication 17 June 2024, date of current version 1 July 2024.

Digital Object Identifier 10.1109/ACCESS.2024.3415731

RESEARCH ARTICLE

Gas Identification Algorithm Based on Dynamic Response Analysis of Metal Oxide Sensors Under Temperature Modulation

YA-HAN FAN[1], TING-I CHOU[1], (Member, IEEE), SHIH-WEN CHIU[2], AND KEA-TIONG TANG[1], (Senior Member, IEEE)
[1]Department of Electrical Engineering, National Tsing Hua University, Hsinchu 30013, Taiwan
[2]Enosim Bio-Tech Company Ltd., Hsinchu 30013, Taiwan

Corresponding author: Kea-Tiong Tang (kttang@ee.nthu.edu.tw)

This work was supported by the National Science and Technology Council (NSTC), Taiwan, under Grant NSTC 113-2218-E-007 -019, Grant MOST 111-2221-E-007-108-MY3, and Grant NSTC 113-2640-E-007 -005.

ABSTRACT Many odors, such as poisonous and exhaust gases, are unsuitable for human detection. Therefore, techniques for predicting gas types and concentrations are essential. The metal oxide sensor utilized in this study is a standard gas sensor due to its excellent stability, affordability, and high sensitivity. However, it does have a drawback: lower selectivity towards different gases. To address this, we employ temperature modulation to enhance the sensor's selectivity. By employing temperature modulation, we can observe the dynamic response of the sensor and capture more features. We utilize low-frequency square wave and triangular wave signals as heating voltages. The former represents rapid heating, while the latter embodies a slower heating process. The objective is to employ these two methods to classify and predict the concentrations of ethanol, methanol, MEK, and ethyl acetate, as well as mixtures of the four gases. Following feature extraction, a neural network is employed for classifying and predicting gas types and concentrations. The results demonstrate a 100% classification accuracy under two different heating voltages. Regarding concentration prediction, using the square wave alone yields an error range of +42.09 to -32.41 and a root mean square error (RMSE) of 4.68%; utilizing the triangular wave alone yields an error range of +13.86 to -18.10 and an RMSE of 4.33%. Employing both waveform types simultaneously results in an error range of +37.97 to -17.48 and an RMSE of 2.91%.

INDEX TERMS Enose, MOX, temperature modulation, gas concentration prediction.

I. INTRODUCTION

A. BACKGROUND

Among the five human senses, smell is one of them. This is through our olfactory organ, the nose, which allows us to perceive odors and distinguish them. This process involves interactions between olfactory receptor cells in the nasal cavity and odorant chemical molecules. When different chemicals in odor enter our nasal cavity, olfactory cells receive the chemical information related to these odor molecules and then convert it into electrical signals, thereby changing the electrical potential. These electrical signals are then transmitted through the olfactory nerve to the olfactory bulb of our brain, which then transmits this information to the brain's olfactory center. People can recognize and understand different smells because we learn and store much smell information in our memory. When we receive different types of smell signals, the brain collects this information and then identifies these smells based on past experiences. However, if we are in an environment full of the same smell for a long time, it can easily lead to olfactory fatigue. In addition, our sense of smell is not always compassionate, and some gases may not be suitable for us to smell in our living environment, such as pungent odors or gases that are harmful to health.

The associate editor coordinating the review of this manuscript and approving it for publication was Ilaria De Munari.

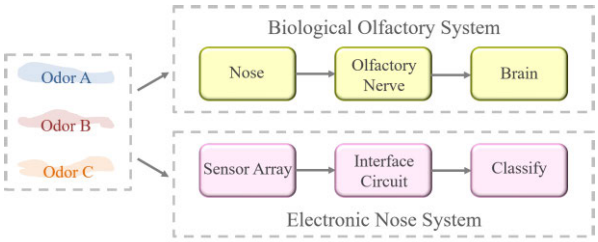

FIGURE 1. Artificial olfactory system.

Therefore, we may need help to sense or identify the types of these gases accurately, and avoiding exposure to toxic gases may be difficult.

Electronic Nose is a bionic olfactory sensing system that senses gases and converts them into electrical signals for analysis and prediction. With the development of science and technology, the application fields of electronic noses are increasingly expanding, such as detecting the breath of patients to determine whether they have lung cancer, detecting the odor released by food to determine whether it has spoiled, identifying drugs, distinguishing the quality of coffee beans, and monitoring air quality. Compared with biological olfactory systems, electronic nose systems can objectively present gas-sensing results and provide more precise analysis. The electronic nose system consists of a sensor array composed of multiple gas sensors to identify odors. The sensor array is like a way that receptor cells change the physical properties of the sensor after contact with odor molecules and capture the surrounding environment. Signals simulate physical changes in neurotransmission, and program algorithms simulate the brain's classification of smells, as shown in Figure 1. Like the human olfactory system, the brain must first learn relevant odor information before identifying odors. Therefore, a corresponding gas database must be established for reference before applying an electronic nose. The electronic nose signal processing process mainly includes data collection, pre-processing, and classification. When the sensor array is exposed to a substance containing an odor, the resistance of the sensor changes depending on the type and concentration of the substance. During the data collection phase, we sample the resistance changes of the gas sensor and establish the sensor's response curve.

B. MOTIVATION

Metal oxide gas sensors have many advantages, including high sensitivity, low cost, and reversibility. However, these sensors need more selectivity, which is also their shortcoming. When we use MOX sensors in gas detection applications, it cannot be easy to differentiate between different gas components. Several approaches were applied to improve the gas and overcome this challenge and selectivity of the sensor. One of them is to increase the number of sensor arrays. Different sensors have different selectivities for different gases, which can help compensate for their shortcomings. Another method is to adjust the film temperature of the metal oxide gas sensor to improve its selectivity for different gases due to different reaction rates at different temperatures. This method is called temperature modulation, which is when we apply different heating voltages to the metal oxide gas sensor. This method will affect the redox rate of the sensor due to different temperatures, so it can obtain different degrees of reactions, thereby improving the gas selectivity of the sensor. Typically, a heating voltage is applied to allow the sensor to reach a stable state before feature acquisition. However, the features that can be captured by this method are limited. In order to improve accuracy and reduce errors further, this paper proposes a new method, namely, the temperature modulation of dynamic reactions. We use varying temperature heating waveforms to heat the sensor and combine multiple waveforms. This dynamic response approach captures more comprehensive features and often helps identify the composition of the target gas, further improving the accuracy of the overall system.

C. REVIEW

In 1989, Sears et al. [10] investigated the conductive response of tin oxide gas sensors subjected to thermal cycling to determine the potential of this technology in enhancing selectivity and sensitivity. When using a shifted sinusoidal waveform to drive the sensor heater, distinct conductivity curves were observed for different gases. The impact of varying reducing gas concentrations on the gas selectivity and the functional relationship between conductivity and gas concentration were further examined, along with the time dependence during the cycle period. In 1991, Wlodek et al. [11] demonstrated the potential applications and limitations of sensor signals with Gaussian functions in the quantitative analysis of binary gas mixtures using a single sensor. It was found that even with a single sensor, the characteristic features of the response waveform components of the mixture could still be retained. In 2004, Huang et al. [12] utilized a single gas sensor based on SnO2 to qualitatively analyze pure pesticide gases and binary gas mixtures in air under a rectangular temperature profile. The experimental results indicated that the sensor achieved high selectivity within the temperature range of 250 to 300°C and a modulation frequency of 20mHz. Quantitative analysis of pure pesticide gases and mixtures was conducted using Fast Fourier Transform (FFT). The higher harmonics of the FFT represented the nonlinear characteristics of the sensor surface response. In 1999, Lee [6] discussed the temperature dependency of sensor conductivity and transient and cyclic modulation techniques employed to enhance the sensitivity and selectivity of sensors in the analysis of single gases and multi-component gas mixtures.

II. STRUCTURE OF THE SYSTEM

A. EXPERIMENTAL SETUP

The experimental setup and process of this study are as follows. First, the sensor array we used in this study has a total of eight sensors, 4 TGS2600 and 4 TGS2611. The reason for using 8 sensors is that using multiple sensors

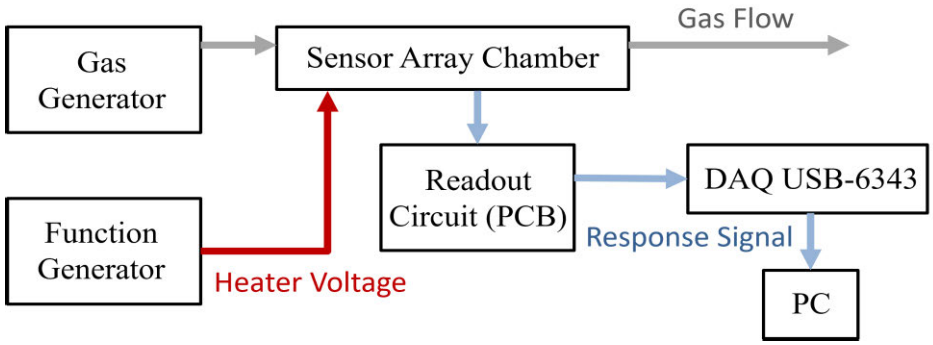

FIGURE 2. Experimental system architecture.

TABLE 1. Experiment setup.

Experiment	
Sensor	Figaro TGS 2611, TGS 2600
Heater Voltage	5mHz 3~5V Square wave, Triangular wave
Experimental gas	Ethanol, 300~900 ppm Methanol, 500~1100 ppm MEK, 900~1500 ppm Ethyl ethanoate, 1300~2000 ppm Ethanol 300~900 ppm and Methanol 400~1100 ppm mixture Ethanol 300~700 ppm and MEK 1000~1900 ppm mixture Methanol 400~900 ppm and MEK 1000~1800 ppm mixture MEK 800~1400 ppm and Ethyl ethanoate 1200~2000 ppm mixture

can produce more features, thereby enhancing accuracy. For instance, while predicting gas concentration with an error of less than 5% using only one sensor is challenging, it can be easily achieved with multiple sensors. And we connect the voltage waveform generated by the function generator to the heater of the sensor for heating. Considering the potential evaporation rate of the simulated liquid in the air, it's plausible that such high concentrations were observed. The gas generator is used to generate gas samples and transport them to the sensor array chamber. At the same time, dry air will be introduced between each experiment to ensure that there will be no residual gas from the previous experiment in the chamber after each experiment. The metal oxide sensor will produce corresponding resistance changes due to oxidation or reduction reactions. The signal acquisition card captures the voltage output in the interface circuit and then transmits the data to the computer for analysis. And Dry air passed through each experimental piece for at least 1000 seconds, and the heater continues to heat while observing the response of the sensor and dry air to ensure that there is no residual target gas.

The gas experiment in this study was completed in a fume hood, and gas samples were generated by a 491MB gas generator (KINTEK). The gas generation method is as follows:

1. Put the liquid state of the target gas into the test tube (the same weight will be measured using a precision balance in each experiment).

2. The output flow rate is fixed at 1L per minute, and the gas generator is set at different temperatures according to the gas to be generated (temperature affects the liquid's evaporation rate, which in turn affects the gas concentration).

3. The volatilized target gas is diluted with dry air and cooled through pipes to room temperature before being outputted to the chamber where the sensor is placed.

4. The sensor response data is read to the computer through the designed PCB board by DAQ USB-6343 at a reading frequency of 10Hz.

B. DATASET

The gas responses collected from gas experiments in this study are shown in Figures 3 and 4. Each pure substance gas and mixed gas has nine concentrations, and each concentration has three pieces of data. The pure substance gas data set and the diverse gas data set each have 108 data.

C. TEMPERATURE MODULATION

The sensor material used in the FIGARO commercial sensors TGS2600 and TGS2611 used in this article is tin dioxide (SnO_2), and the two main chemical reactions on the sensor are oxidation and reduction. When oxygen in the gas forms chemically adsorbed ions on the surface of the metal oxide, it interacts with electrons at the same time, causing the conductivity of the material to weaken:

$$O_2\,(Gas) + 2e^- \longrightarrow 2\,O^-, \tag{1}$$

When the adsorbed oxygen ions react with the reducing gas, the reducing gas reacts with the adsorbed oxygen ions at the same time and releases the previously bonded free electrons, thereby improving the conductivity of the material:

$$O^- \mp R\,(Gas) \rightarrow RO\,(Gas) + e^-, \tag{2}$$

When using a square wave, at the moment when the voltage is converted from 3V to 5V, that is, the sensing material receives the instantaneously increased heating voltage and heats up instantly. At this moment, the reaction rate of Equation 3.2 will be increased instantaneously, thus suddenly reflecting a large number of free electrons, so that Conductance suddenly rises. When using a triangle wave, the conductance of the sensor will increase until the temperature reaches the optimal catalytic oxidation temperature [10], and then begin to decrease.

In the process of temperature modulation, temperature changes will affect the reaction rate [24] because the reaction rate is closely related to temperature. As the temperature changes, the corresponding electron concentration will also vary. Such dynamic changes cause different target gases to have different reaction constants and reaction formulas in this process. Due to this difference, we can observe that different gases exhibit completely different reaction characteristics when the temperature changes, forming their unique waveforms. This characteristic waveform can be considered a unique indicator of each gas, reflecting its unique reaction behavior at different temperatures. We can effectively classify different gases through in-depth analysis of these characteristic waveforms.

D. DATA READOUT

In this experiment, we used the circuit schematic on the TGS2611 sensor provided by Figaro. While conducting this experiment, we fixed V_C at 5V while adjusting V_H to vary the heater power. This operation is to obtain the sensor resistance value R_S, which is achieved by using another resistor R_L to obtain the divided voltage V_{out}. When the sensor detects the presence of gas, it will cause R_S to drop, thereby causing the output voltage V_{out} to rise. This can be described by the following formula:

$$R_S = R_L \times \frac{5 - V_{out}}{V_{out}}, \tag{3}$$

In this experiment, given that the sensor's responses manifest as continuous analog signals, we utilized the DAQ USB-6343 to convert these analog signals into digital format. Such conversion enables subsequent data processing and analysis to be conducted with greater convenience. Specifically, we opted to capture signals at a sampling frequency of 10Hz. On the computer end, we employed the Signal Express software developed by National Instruments to receive the DAQ signal. This software offers an intuitive and user-friendly interface, facilitating efficient signal acquisition. Following acquisition, we access the obtained signals on the computer for further in-depth analysis.

III. METHODS

A. FEATURE EXTRACTION

When using square waves and triangle waves as the heating voltage of the system, we used a wave with a frequency of 5mHz, that is, a period of 200 seconds, so we will also get a response of 200 seconds. The reaction rate between gas and sensor material will be different at different temperatures, thus affecting sensitivity. After observing the square wave heating process, we found the response most apparent when the heating voltage increased instantaneously. Therefore, when using square wave heating voltage, we will take 50 seconds from the moment the temperature rises as the characteristic. After observing the triangular wave heating, we found that the response was apparent when the heating voltage increased. Therefore, when using the triangular wave heating voltage, we will take the 20th to 70th second of the rising band of the triangular wave as the characteristic. The acquisition frequency I used is 10Hz, so there will be 500 data points for a set of features. The gas chamber in the experimental setup of this article is a chamber with a sensor array formed by eight sensors, so a piece of data will have 4,000 data points.

B. PURE GAS ANALYSIS BASED ON MACHINE LEARNING

The part about pure gases is divided into classification of gas types and prediction of gas concentration. Among them, several methods are used to classify gases, which will be introduced one by one below. Firstly, the extracted features are meticulously sorted out one by one, paving the way for the initiation of experiments employing the traditional machine learning model, Support Vector Machine (SVM). SVM, a supervised learning algorithm renowned for its prowess in classification and regression tasks, is employed here to discern patterns within the dataset. At its core, SVM endeavors to identify an optimal hyperplane that effectively delineates data points across different categories. Notably, SVM is adept at handling nonlinear data by mapping it to a higher-dimensional space using kernel functions, thereby facilitating more effective data separation. Given that the original feature data boasts high dimensionality, ranging from 4000 to 8000 dimensions, a preprocessing step involving Principal Component Analysis (PCA) is enacted. PCA serves the dual purpose of dimensionality reduction and feature transformation, condensing the data into a more manageable and representative four-dimensional space. This strategic maneuver enhances the model's efficacy in grappling with the intricacies of the four pure substance gases intrinsic to the experimental data. Subsequently, SVM is deployed for further classification operations, leveraging the insights gleaned from the preprocessed data. The dataset is partitioned into training and testing subsets, with 80% of the data earmarked for training purposes and the remaining 20% reserved for assessing the model's predictive prowess. Impressively, the classification accuracy attains a perfect score of 100%, underscoring the efficacy of SVM in discerning distinctive patterns within the dataset and accurately classifying data points.

The gas concentration prediction model utilizes XGBoost (eXtreme Gradient Boosting) as its core algorithm. XGBoost, tailored for regression tasks, employs a gradient boosting framework, amalgamating multiple decision trees to construct a robust predictive model. This iterative optimization process continually enhances prediction accuracy by minimizing the square loss function, ensuring precise numerical predictions. To mitigate overfitting, regularization techniques are employed, ensuring the model not only fits the training data but also generalizes well to unseen data, thereby enhancing prediction accuracy for new data instances. Employing this approach, the root mean square error (RMSE) is calculated as 3.865% for the square wave, 3.758% for the triangular wave, and 2.581% when both waveforms are

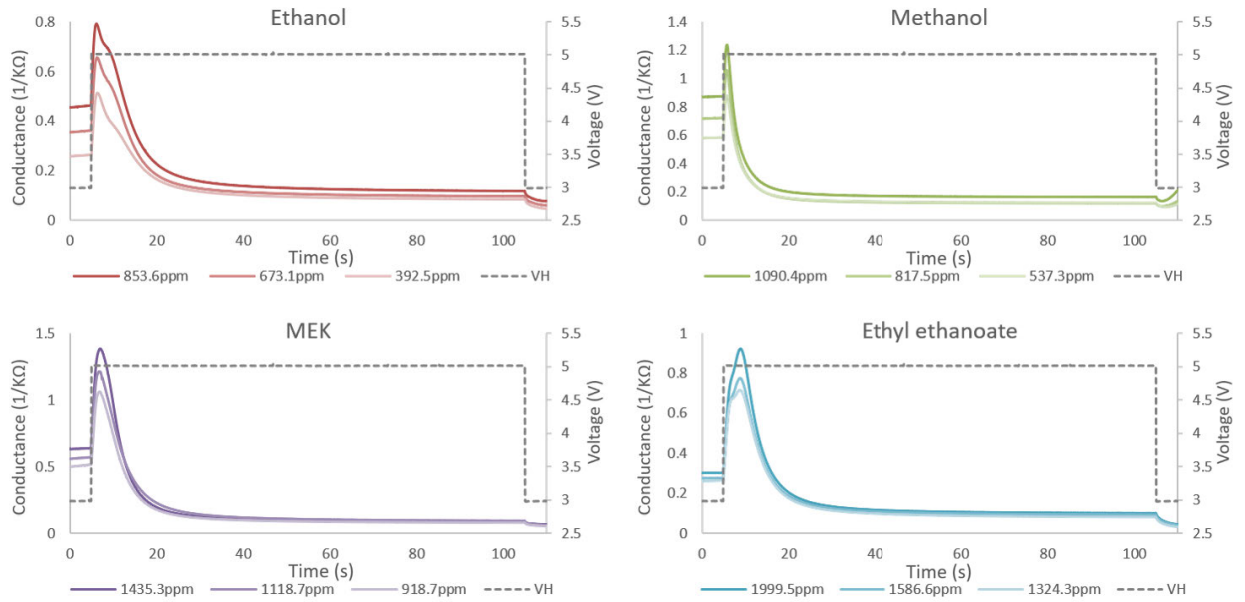

FIGURE 3. Square wave gas response.

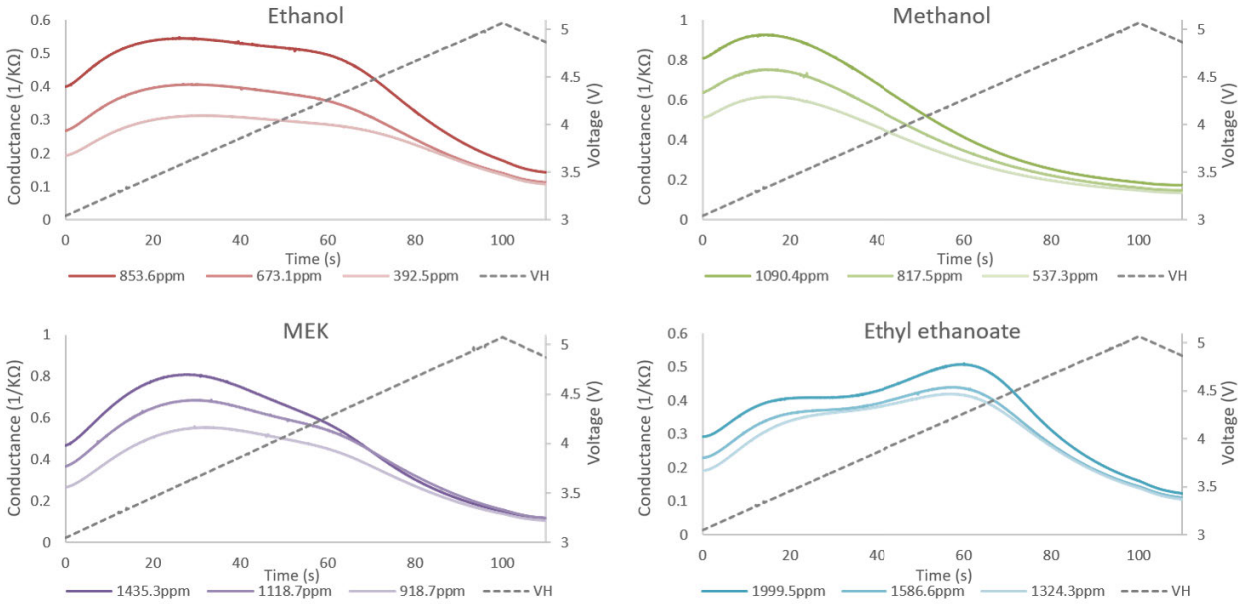

FIGURE 4. Triangular wave gas response.

utilized simultaneously. This predictive framework, rooted in XGBoost, underscores its versatility in handling regression challenges, leveraging a sophisticated ensemble of decision trees to refine prediction accuracy iteratively. Through meticulous optimization via gradient boosting, it adeptly minimizes prediction errors, thereby furnishing a reliable model for gas concentration forecasting. Furthermore, the incorporation of regularization techniques serves to fortify the model against overfitting, ensuring its applicability across diverse datasets. The calculated RMSE values attest to the efficacy of this approach, highlighting its adeptness in capturing the nuances of square and triangular waveforms, and their combined effect, with remarkable precision.

C. GAS MIXTURE ANALYSIS

In the mixed gas analysis part, because the components are relatively complex, we want to use multiple regression and projection methods to predict various concentrations in the early stage. We first use the data of pure substance gases to find four regression equations and then input the mixed gas data for prediction. However, due to the complex composition of the mixed gas, after trying to use several mixing models,

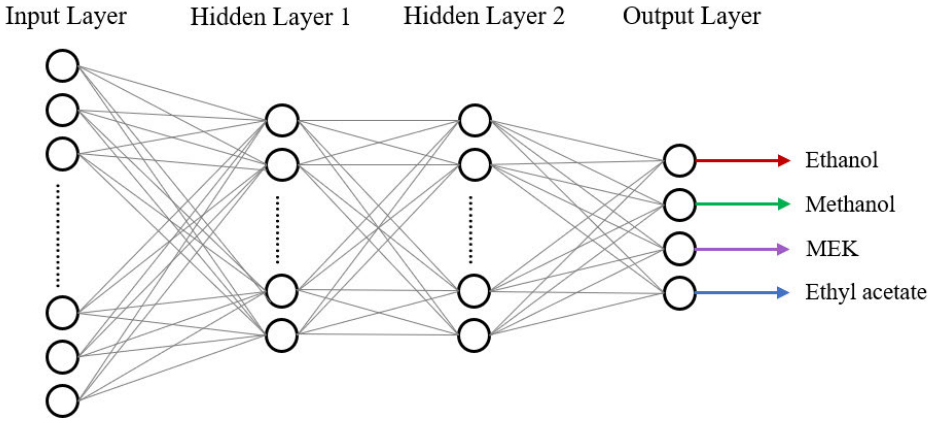

FIGURE 5. Neural network diagram.

it was found that the error was high and the effect was not ideal. It is speculated that because mixed gases are much more complex than pure gases, using traditional machine learning may not yield good results. In my previous experiments, relying solely on machine learning methods may lead to errors exceeding 20%. Recognizing the urgent need to minimize error rates, this study is committed to implementing advanced methods tailored for analyzing mixed gases. Therefore, a neural network was used to classify the gas and predict the concentration of each component for analysis.

The data set is divided into a training set at a ratio of 80% and a test set at a ratio of 20%. Then, a neural network model was established. The model included four layers. The number of neurons in each layer was 4000, 400, 40 and 4 respectively. The activation functions of the input layer and the two hidden layers were ReLU (Rectified Linear Unit):

$$f(x) = \max(0, x), \tag{4}$$

The activation function of the output layer is Linear:

$$f(x) = x, \tag{5}$$

Subsequently, the model is compiled, and the Adam optimizer update rule is used to include the first moment and second moment of the gradient:

1. Update of First Moment:

$$m_t = \beta_1 \cdot m_{t-1} + (1-\beta_1) \cdot g_t, \tag{6}$$

m_t is the first moment at time step t, g_t is the gradient, and β_1 is a decay parameter between 0 and 1.

2. Update of Secon Moment:

$$v_t = \beta_2 \cdot v_{t-1} + (1-\beta_2) \cdot (g_t)^2, \tag{7}$$

v_t is the second-order momentum at time step t, and β_2 is a decay parameter between 0 and 1.

3. Corrected first-order momentum and second-order momentum:

$$\hat{m}_t = \frac{m_t}{1-\beta_1^t} \tag{8}$$

$$\hat{v}_t = \frac{v_t}{1-\beta_2^t}, \tag{9}$$

4. Update the weight formula:

$$\theta_t + 1 = \theta_t - \frac{\eta}{\sqrt{\hat{v}_t} + \epsilon} \cdot \hat{m}_t, \tag{10}$$

θ_t is the parameter, η is the learning rate, and ϵ is the decimal added to stabilize the division. By calculating first moment and second moment, combined with adaptive learning rate, and making corrections on each parameter, the training effect is improved.

During the training phase, 20% of the data is retained as the validation set as described previously. Finally, use the trained model to predict on the test set, and calculate the root mean squared error of the prediction results. When the two waveforms are used together, the input layer of the neural network is adjusted to 8000 neurons.

Given that all pure material gas components constitute potential elements of the mixed gas, both the pure material gas data and the mixed gas data are concurrently fed into a unified neural network for concentration prediction. This approach leverages the inherent relationships between the individual gas components and their collective presence within the mixed gas environment. Upon conducting concentration predictions using the aforementioned neural network, the resulting root mean square errors (RMSE) are obtained. Specifically, utilizing the square wave as the heating voltage yields an RMSE of 69.39 parts per million (ppm), while employing the triangular wave yields an RMSE of 38.68 ppm. Notably, combining both waveforms culminates in a reduced RMSE of 23.33 ppm. This comprehensive analysis underscores the efficacy of integrating diverse data sources and waveform inputs to enhance the accuracy of gas concentration predictions, thereby advancing the understanding and application of predictive models in gas sensing technologies.

In this study, the way to express the concentration prediction error is by using the root mean squared error as shown in the formula:

$$\textit{root mean squared error}(ppm) = \sqrt{\frac{\sum_l^n \left(y_{predict_i} - y_{true_i}\right)^2}{n}}, \tag{11}$$

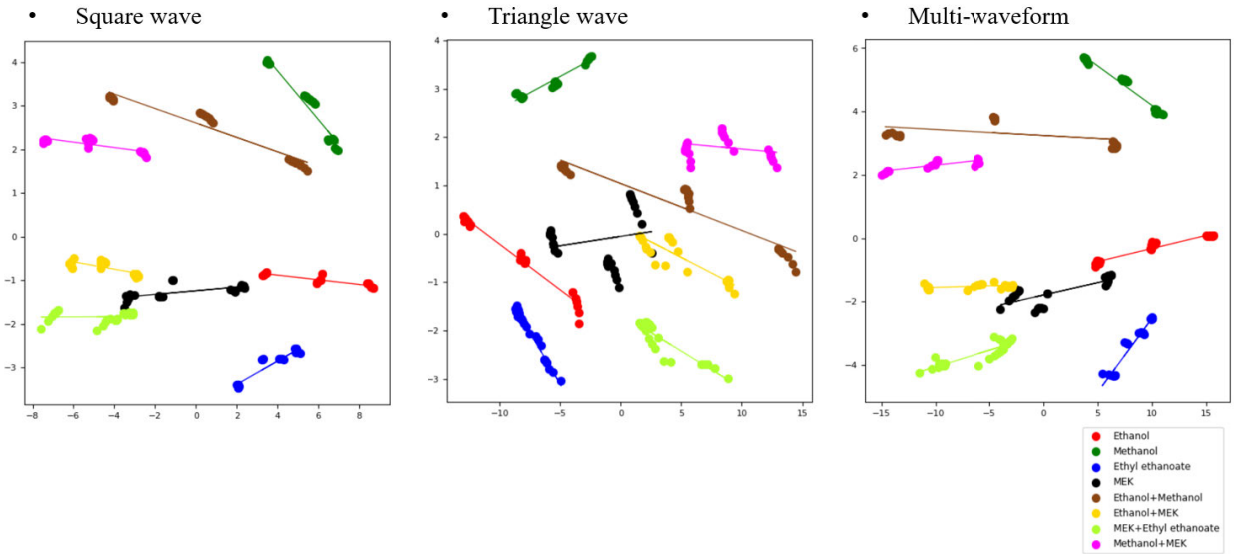

FIGURE 6. PCA plot of mixed gas.

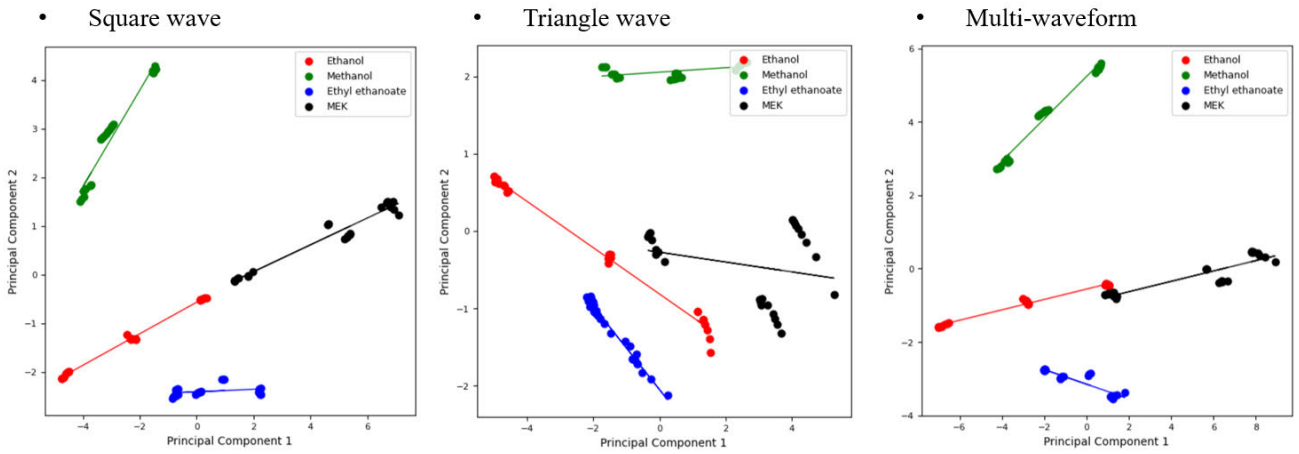

FIGURE 7. PCA plot of pure gas.

Following the utilization of the neural network for predicting the concentrations of the four gases, the ensuing step involves employing a specific formula to compute the errors. Given that the mixed gas constitutes a binary mixture, wherein the concentrations of two out of the four gases are expected to be 0 parts per million (ppm), it becomes imperative to calculate the error. However, due to the inability to calculate percentage errors in scenarios where the denominator is 0, the concentration value itself is utilized to express the error. This pragmatic approach allows for a meaningful assessment of prediction accuracy despite the inherent complexities associated with binary mixtures.

IV. EXPERIMENTAL RESULT

From the feature extraction phase, it becomes evident that each gas exhibits a unique response pattern in reaction to both the instantaneous heating of the square wave and the gradual heating of the triangular wave. To facilitate visual comprehension, I initially subjected the extracted feature dataset of pure material gases to dimensionality reduction using Principal Component Analysis (PCA). This process transforms the dataset into a visually comprehensible form, enabling us to discern characteristic differences among the gases more intuitively. The resulting figure below illustrates the characteristic data post-PCA dimensionality reduction. Notably, each gas manifests along a regression line, forming distinct clusters corresponding to varying concentrations.

Subsequently, the dimensionality reduction process utilizing Principal Component Analysis (PCA) was applied to the extracted mixed gas feature dataset to visually represent the features. Nevertheless, observations derived from the plots following PCA dimensionality reduction unveil a complexity in the gas mixture that surpasses initial expectations. Despite successfully establishing regression lines, visual inspection reveals a notable dispersion among many data points, with some nearly overlapping. Therefore, in order to delve deeper into the analysis and interpretation of this intricate data, neural networks are employed to analyze mixed gases.

TABLE 2. Error comparison.

	Square	Triangle	Square + Triangle
RMSE without y_real=0	4.68 %	4.33%	2.91 %
Error for y_real=0 (ppm)	42.09 ~ -32.41	13.86 ~ -18.10	37.97 ~ -17.48

TABLE 3. Comparison table.

	[7]	[8]	[25]	This Work
Target Gas Type	Acetone, Ethanol	Ethanol, Methanol	Acetone, Ethanol, Methanol	Ethanol, Methanol, MEK, Ethyl ethanoate
Target Gas Concentration	0~40 ppm	100~800 ppm	28~85 ppm	300~2000 ppm
Gas Sensor Type	MOX	MOX	Conducting Polymer	MOX
Heating Type	Dual-temperature mode	Square wave, Triangle wave	N/A	Square, Triangle wave, Multi-waveform
Error (ppm)	0.67 ppm	N/A	5~20 ppm	23.33 ppm
Error (%)	N/A	12.6 %	N/A	2.91 %

The rmse (room mean square error) calculated by XGBoost is 3.865% for the square wave, 3.758% for the triangle wave, and 2.581% when using multi-wave.

The concentration prediction results obtained through neural networks are presented herein. Due to potential instances where calculating error percentages might entail division by zero, two distinct methodologies are employed for error calculation. One method involves expressing errors as concentration values, while the other computes error percentages while excluding actual values of 0. When utilizing the square wave alone, the error range spans from +42.09 to -32.41, with a corresponding root mean square error (RMSE) of 4.68%. Similarly, employing the triangular wave in isolation yields an error range of +13.86 to -18.10, with an RMSE of 4.33%. Remarkably, employing both waveform types simultaneously results in a narrower error range of +37.97 to -17.48 and a reduced RMSE of 2.91%, as shown in Table 2.

V. CONCLUSION

For pure material gases, due to their simple composition, SVM classification can achieve 100% classification accuracy whether using square waves or triangular waves alone or using both wave types together. When using XGBoost to predict the concentration of pure substance gases, although the rmse of using square wave or triangle wave alone or using two wave types together falls within 4%, it can be found that the error reaches the lowest when using two wave types together. 2.581%.

For mixed gases, we finally decided to use neural networks for analysis because of the complex composition. We also used square waves, triangle waves, and neural networks with two wave types to make concentration predictions. However, the method will appear in some data. Dividing by 0 is an error, so there are two items in the error comparison, one is the concentration rmse error value, and the other is the error percentage that excludes the actual value of 0 in the data. In this method, although the minimum concentration rmse positive error value appears when using only the triangle wave, the minimum concentration rmse negative error value and the minimum error percentage both appear in the prediction results when two wave types are used together, so I judge that two types of heating are used at the same time. Voltage and extracting features for analysis will give better results.

According to the results of this study, it was observed that whether XGBoost or neural network is used to predict gas concentration, the waveforms using two temperature modulations perform better than a single waveform. The reason behind this result is that the use of temperature modulation, whether it is a square wave that heats up quickly or a triangle wave that heats up slowly, can generate more usable information. Combining the square wave and triangular wave signals enriches the composition of the obtained feature dataset, thereby enhancing the breadth and depth of information available for analysis. By integrating these two distinct heating methodologies, we augment the diversity of features captured from the sensor's dynamic response. The rapid heating of the square wave signal and the gradual heating characteristic of the triangular wave signal evoke different responses from the sensor, unveiling nuanced insights into the gas-sensing process. This amalgamation of waveform types not only broadens the scope of features extracted but also facilitates a more comprehensive understanding of the sensor's behavior across varying conditions and gas compositions. This enables the prediction model to more comprehensively capture the characteristics of gas concentration changes, thereby achieving lower errors than a single wave pattern. Table 3 shows the comparison of this study with other literature. Compared with [8] that uses a single heating wave pattern, this study enables multiple heating wave lines to effectively reduce errors. Compared with [25] which only uses machine learning, the error percentage is also effectively reduced. By combining square wave and triangle wave temperature modulation methods, we successfully created a more diverse feature data set, which makes the prediction model more adaptable and accurate. The synergy between the two makes the prediction results more reliable and helps improve the performance of the overall detection system.

REFERENCES

[1] A. Perera, A. Pardo, D. Barrettino, A. Hierlermann, and S. Marco, "Evaluation of fish spoilage by means of a single metal oxide sensor under temperature modulation," *Sens. Actuators B, Chem.*, vol. 146, no. 2, pp. 477–482, Apr. 2010.

[2] X. Huang, F. Meng, Z. Pi, W. Xu, and J. Liu, "Gas sensing behavior of a single tin dioxide sensor under dynamic temperature modulation," *Sens. Actuators B, Chem.*, vol. 99, nos. 2–3, pp. 444–450, May 2004.

[3] W. Göpel and K. D. Schierbaum, "SnO_2 sensors: Current status and future prospects," *Sens. Actuators B, Chem.*, vol. 26, nos. 1–3, pp. 1–12, Jan. 1995.

[4] S. Aymen, G. Besnard, P. Menini, C. Talhi, F. Blanc, B. Franc, M. L. Kahn, K. Fajerwerg, and P. Fau, "Detection and discrimination methods of sub-ppm nitrogen dioxide (NO_2) with a copper oxide sensor operated with a pulsed temperature modulation," *Sensors Transducers*, vol. 222, no. 6, pp. 24–30, 2018.

[5] N. Barsan, D. Koziej, and U. Weimar, "Metal oxide-based gas sensor research: How to?" *Sen. Actuators B, Chem.*, vol. 121, no. 1, pp. 18–35, 2007.

[6] A. Lee, "Temperature modulation in semiconductor gas sensing," *Sens. Actuators B, Chem.*, vol. 60, no. 1, pp. 35–42, Nov. 1999.

[7] S. Madrolle, P. Grangeat, and C. Jutten, "A linear-quadratic model for the quantification of a mixture of two diluted gases with a single metal oxide sensor," *Sensors*, vol. 18, no. 6, p. 1785, Jun. 2018.
[8] W.-C. Wen, Y.-T. Liu, and K.-T. Tang, "Gas mixture analysis based on metal-oxide semiconductor gas sensors with temperature modulated method," in *Proc. IEEE Int. Symp. Olfaction Electron. Nose (ISOEN)*, May 2019, pp. 1–4.
[9] *FIGARO USA*. Accessed: Jan. 9, 2024. [Online]. Available: http://www.figarosensor.com/
[10] W. M. Sears, K. Colbow, and F. Consadori, "General characteristics of thermally cycled tin oxide gas sensors," *Semicond. Sci. Technol.*, vol. 4, no. 5, pp. 351–359, May 1989.
[11] S. Wlodek, K. Colbow, and F. Consadori, "Signal shape analysis of a thermally cycled tin oxide gas sensor," *Sens. Actuators B, Chem.*, vol. 3, no. 1, p. 6368, 1991.
[12] X. Huang, L. Wang, Y. Sun, F. Meng, and J. Liu, "Quantitative analysis of pesticide residue based on the dynamic response of a single SnO_2 gas sensor," *Sens. Actuators B, Chem.*, vol. 99, nos. 2–3, pp. 330–335, May 2004.
[13] D. Zhang, J. Liu, C. Jiang, A. Liu, and B. Xia, "Quantitative detection of formaldehyde and ammonia gas via metal oxide-modified graphene-based sensor array combining with neural network model," *Sens. Actuators B, Chem.*, vol. 240, pp. 55–65, Mar. 2017.
[14] M. A. Ryan, H. Zhou, M. G. Buehler, K. S. Manatt, V. S. Mowrey, S. P. Jackson, A. K. Kisor, A. V. Shevade, and M. L. Homer, "Monitoring space shuttle air quality using the jet propulsion laboratory electronic nose," *IEEE Sensors J.*, vol. 4, no. 3, pp. 337–347, Jun. 2004.
[15] E. Martinelli, D. Polese, A. Catini, A. D'Amico, and C. Di Natale, "Self-adapted temperature modulation in metal-oxide semiconductor gas sensors," *Sens. Actuators B, Chem.*, vol. 161, no. 1, pp. 534–541, Jan. 2012.
[16] L.-Y. Chen, C.-C. Wu, T.-I. Chou, S.-W. Chiu, and K.-T. Tang, "Development of a dual MOS electronic nose/camera system for improving fruit ripeness classification," *Sensors*, vol. 18, no. 10, p. 3256, Sep. 2018.
[17] R. M. Schnabel, M. L. L. Boumans, A. Smolinska, E. E. Stobberingh, R. Kaufmann, P. M. H. J. Roekaerts, and D. C. J. J. Bergmans, "Electronic nose analysis of exhaled breath to diagnose ventilator-associated pneumonia," *Respiratory Med.*, vol. 109, no. 11, pp. 1454–1459, Nov. 2015.
[18] L. T. Tanoue, "Detection of lung cancer by sensor array analyses of exhaled breath," *Yearbook Pulmonary Disease*, vol. 2007, pp. 136–138, Jan. 2007.
[19] K.-T. Tang, Y.-S. Lin, and J.-M. Shyu, "A local weighted nearest neighbor algorithm and a weighted and constrained least-squared method for mixed odor analysis by electronic nose systems," *Sensors*, vol. 10, no. 11, pp. 10467–10483, Nov. 2010.
[20] J. J. Moré, "The Levenberg–Marquardt algorithm: Implementation and theory," in *Numerical Analysis*. Berlin, Germany: Springer, 1978, pp. 105–116.
[21] K. A. Ngo, P. Lauque, and K. Aguir, "High performance of a gas identification system using sensor array and temperature modulation," *Sens. Actuators B, Chem.*, vol. 124, no. 1, pp. 209–216, Jun. 2007.
[22] W. Wang and Y.-M. Zhang, "Application of recursive predict error neural networks in mechanical propertise forecasting," in *Proc. Int. Joint Conf. Artif. Intell.*, Apr. 2009, pp. 132–135.
[23] A. Fort, M. Gregorkiewitz, N. Machetti, S. Rocchi, B. Serrano, L. Tondi, N. Ulivieri, V. Vignoli, G. Faglia, and E. Comini, "Selectivity enhancement of SnO_2 sensors by means of operating temperature modulation," *Thin Solid Films*, vol. 418, no. 1, pp. 2–8, Oct. 2002.
[24] V. Lantto, "Semiconductor gas sensors based on SnO_2 thick films," in *Gas Sensors: Principles, Operation and Developments*. Dordrecht, The Netherlands: Springer, 1992, pp. 117–167.
[25] Y. S. Lin, "Method on odor analysis for electronic nose system," M.S. thesis, 2009.
[26] Y.-H. Fan, T.-I. Chou, S.-W. Chiu, and K.-T. Tang, "Gas prediction method based on dynamic response analysis of metal oxide sensors under temperature modulation," in *Proc. IEEE SENSORS*, Oct. 2023, pp. 1–4.
[27] C. Kervazo and J. Bobin, "Sequential sparse blind source separation for non-linear mixtures," *J. Phys., Conf.*, vol. 1476, no. 1, Mar. 2020, Art. no. 012008.
[28] P. Grangeat, M.-P. Duval Comsa, A. Koenig, and R. Phlypo, "Dynamic modeling of carbon dioxide transport through the skin using a capnometry wristband," *Sensors*, vol. 23, no. 13, p. 6096, Jul. 2023.
[29] W.-J. Zhao, K.-L. Ding, Y.-S. Chen, F.-Y. Xie, and D. Xu, "Optimized low frequency temperature modulation for improving the selectivity and linearity of SnO_2 gas sensor," *IEEE Sensors J.*, vol. 20, no. 18, pp. 10433–10443, Sep. 2020.

YA-HAN FAN received the B.S. degree in engineering and system science from National Tsing Hua University, Hsinchu, Taiwan, in 2021, where she is currently pursuing the M.S. degree in electrical engineering. Her research interests include gas identification algorithms and Enose systems.

TING-I CHOU (Member, IEEE) received the B.S. degree in electrical engineering from National Tsing Hua University, Hsinchu, Taiwan, in 2013, where he is currently pursuing the Ph.D. degree. His research interests include Enose systems, drift calibration algorithms, and bio/chemical SoC design.

SHIH-WEN CHIU received the B.S. degree in electrical engineering from National Central University, Zhongli, Taiwan, in 2007, and the M.S. and Ph.D. degrees, in 2009 and 2014, respectively. He was a Postdoctoral Research Fellow in electrical engineering with National Tsing Hua University, Hsinchu, in 2014. He is currently the Founder and the CEO of the start-up company, Enosim Bio-Tech Company Ltd. His research interests include bio-inspired gas sensing systems, bio/chemical SoC design, and mixed-mode IC design.

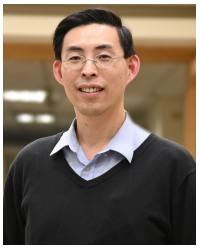

KEA-TIONG TANG (Senior Member, IEEE) received the B.S. degree in electrical engineering from National Taiwan University, Taipei, Taiwan, in 1996, and the M.S. and Ph.D. degrees in electrical engineering from California Institute of Technology, Pasadena, CA, USA, in 1998 and 2001, respectively.

From 2001 to 2006, he was a Senior Electrical Engineer with Second Sight Medical Products, Inc., Sylmar, CA, USA. He designed mixed-signal ASIC for the Argus®II Retinal Prosthesis System, which became the first FDA-approved device for retinal prosthesis. Since 2006, he has been with the Electrical Engineering Faculty, National Tsing Hua University, Hsinchu, Taiwan, where he is currently a Full Professor. He has led the largest electronic nose team in Taiwan to develop a system that can early detect and rapidly diagnose ventilator-associated pneumonia. His research interests include bio-inspired learning chips, miniature electronic systems, and biomedical implantable prosthetic devices. He has actively collaborated with researchers in nanoengineering and microsystems, chemistry, computer science, electrical engineering, life science, and medical doctors. He has published more than 180 peer-reviewed journal articles and conference papers in these research areas.

Dr. Tang is a member of IEEE SSCS, CASS, EDS, and EMBS. He has served as a TPC Member for ISSCC, IEDM, ASSCC, ISCAS, and BioCAS. He was a recipient of numerous awards, including the Outstanding Young Scholar Award, the Wu Ta-You Memorial Award, the National Innovation Award, and the Outstanding Electrical Engineering Professor Award. He was the Past Chair of the IEEE Biomedical and Life Science Circuits Systems Technical Committee (BioCAS). He was the IEEE CAS Chapter Chair of Taipei Section, from 2017 to 2018. He is the Chair of the IEEE Taipei Section. He is the current Editor-in-Chief of IEEE TRANSACTIONS ON BIOMEDICAL CIRCUITS AND SYSTEMS. He was a Board of Governor (BoG) of the CAS Society, serving as a Representative of Region 10 (2020–2021). He is the current Vice President of Regional Activities and Membership of IEEE CASS.